Sedimentology (2000) **47,** 1039–1051

Open-coast intertidal deposits and the preservation potential of individual laminae: a case study from east-central China

CONGXIAN LI*, PING WANG†[1], FAN DAIDU*, DANG BING* and LI TIESONG*
**Marine Geology Laboratory, Tongji University, Shanghai 200092, China (E-mail: cxlik@online.sh.cn)*
†Coastal Studies Institute, Louisiana State University, Baton Rouge, LA 70803, USA (E-mail: pwang2@unix1.sncc.lsu.edu)

ABSTRACT

Monitoring of sedimentation and erosion was conducted on an open coastal tidal flat on the southern flank of the Yangtze delta. Various elevation references were established in the intertidal zone and monitored intensively for 4 months in order to examine fortnightly and seasonal (calm weather and storm season) sedimentation and erosion. Longer term (100 years) sedimentation and preservation were investigated through examination of cores and trenches. Two different vertical grouping patterns of tidal bedding were distinguished with thinner and thicker sandy laminae. The number of sand-dominated layers and individual muddy and sandy lamina in the cores were compared with theoretically derived sedimentation rates in order to assess long-term preservation potential. Waves, especially high storm waves, have a significant influence on sedimentation and the preservation of intertidal deposits along the open-coast tidal flat. Monitoring during one season indicated that the sand-dominated layer was directly related to storm deposits, while the mud-dominated layer was deposited during calm weather conditions. The variation in sandy lamina thickness was not related to spring–neap tidal cycles during the monitoring period. The assumption of 100% preservation of sandy laminae deposited during every tidal cycle, which has been assumed in previous time-series analyses for the identification of palaeotidal periodicity, was found to be unrealistic along this open-coast tidal flat. Preservation potential decreases as temporal scale increases. During one neap–spring tidal cycle, the preservation potential of individual sandy and muddy laminae was of the order of 10%. Over a period of 100 years, the estimated preservation potential of individual laminae, including both calm weather and storm deposits, decreased to 0·2%. The 100-year preservation potential of storm-induced, sand-dominated layers was estimated to be of the order of 10%.

Keywords Preservation potential, sedimentary structures, sedimentation rate, storm deposits, tidal-flat deposits, Yangtze delta.

INTRODUCTION

Studies of modern tidal bundles (Boersma, 1969; Boersma & Terwindt, 1981) and sedimentation characteristics during neap–spring tidal cycles (Visser, 1980) have provided a potential tool for identifying the periodicity of palaeotides and the estimation of palaeosedimentation rates. The original studies on modern tidal bundles (Boersma, 1969) and neap–spring tidal cycles (Visser, 1980) were mostly conducted in tidal channels. A time-series analysis of the variation in tidal-bundle thickness was developed by Yang & Nio (1985) on the assumption that tidal deposits should be periodic and storm deposits should be random. A 100% preservation potential was

[1]*Corresponding author.*

implied in this time-series analysis, as hiatuses caused by erosion, which are probably random, were not considered. The Yang & Nio (1985) method provided a possible tool for identifying various tidal periodicities and random storm influences. Such time-series analysis of laminae thickness has been applied in studies on ancient tidal deposits to quantify palaeotide periodicity and palaeosedimentation rate (e.g. Tessier & Gigot, 1989; Tessier, 1993; Kvale *et al.*, 1989; Kuecher *et al.*, 1990; Kvale & Archer, 1990; Miller & Eriksson, 1997), and an approximate 14-day periodicity of spring and neap tides has been identified in most of these studies. It is generally accepted that thick sand laminae correspond to relatively higher energy events, typically explained as individual tides during spring tide conditions, while thin sand laminae correspond to relatively low-energy events, such as individual tides during neap tides (Allen, 1985). It is worth noting that Allen's (1985) theoretical model considers temporal lamina thickness variations at a fixed location. The thickness of tidal laminae may also vary from upper tidal flat to lower tidal flat on account of the different intensities of waves and currents.

In this study, a stretch of open-coast tidal flat from the southern flank of the modern Yangtze delta was examined. Sediment grain size was analysed, and numbers of tidal laminae were counted in three cores and one trench. Measurements of relative tidal-flat elevation were conducted during May–September 1992, and the influence of typhoons was studied by comparing tidal-flat conditions both before and shortly after their impact. In this manner, the short-term preservation potential of calm weather tidal bedding was estimated, and the characteristics of storm-induced erosion and deposition were examined. The objective of the present study is to identify the influence of the erosional hiatus induced by waves, especially storm waves, on the determination of tidal periodicity and sedimentation rate along an open-coast tidal flat.

STUDY AREA

The Yangtze River discharges into the East China Sea in a belt of tectonic subsidence (Li *et al.*, 1991). The river carries an average annual sediment discharge of approximately $5{\cdot}0 \times 10^{11}$ kg, the second greatest in China after the Yellow River. The Yangtze River enters the eastern coastal plain from the hilly area in the vicinity

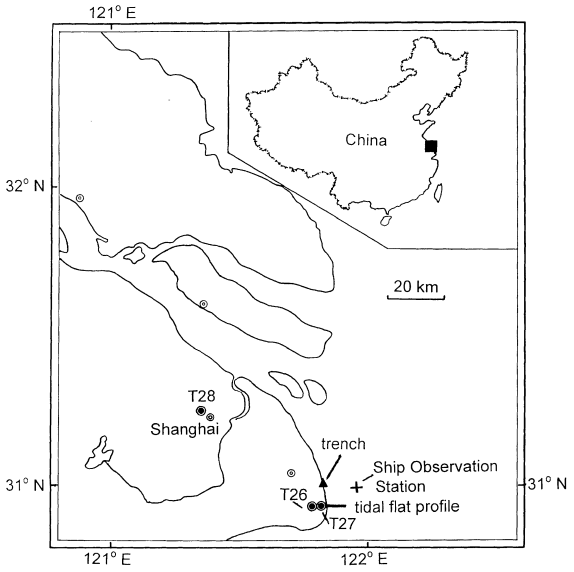

Fig. 1. The study area with locations of the cores, trench and the intertidal profile.

of Zhenjiang and Yangzhou, forming the Holocene delta (Fig. 1). The delta covers an area of approximately 52 000 km^2, with 23 000 km^2 being subaerial and 29 000 km^2 subaqueous (Li *et al.*, 1979). Tidal-flat deposits, including those in supratidal, intertidal and subtidal zones, cover a large area of the subaerial delta. Sediment is composed predominantly of silt, with fine sand being the coarsest grain size. Clay content ranges from 4% to 25% (Li, 1986).

The average semi-diurnal tidal range at the mouth of the Yangtze River is 2·6 m, with a maximum spring tidal range of 4·5 m (Chen, 1998). The tidal flat faces the open East China Sea, which has a continental shelf more than 400 km in width. The flood and ebb tidal currents are not influenced by tidal channels, which are absent in the study area.

Wave energy is typically low and significantly dissipated across the broad flat during calm weather. Field observation indicates that wave energy is generally higher in the sandier upper subtidal to lower intertidal zones compared with that in the muddier mid- to upper intertidal zones. High wave energy is typically associated with the passage of typhoons and strong tropical cyclones. Waves as high as 6 m were recorded at the Ship Observation Station (Fig. 1) located approximately 14 km east of the study area in a water depth of 14–17 m (Zhu *et al.*, 1989). Wave heights, at 0·5 m increments, are estimated visually every 6 h (Sun, 1981). During the summer, over 70% of the waves are from the SE quadrant,

Table 1. Average summer and winter wave conditions at the Ship Observation Station in the Yangtze river mouth, averaged from 1965 to 1992.

	Summer (July)			Winter (January)		
Direction	Frequency of occurrence (%)	Maximum wave height (m)	Average wave height (m)	Frequency of occurrence (%)	Maximum wave height (m)	Average wave height (m)
N	–	1·5	0·8	25·4	2·7	1·0
NNE	–	2·4	0·7	18·2	3·4	1·3
NE	–	1·8	0·8	11·8	3·1	0·8
NEE	–	3·2	0·8	5·9	1·6	0·6
E	6·4	3·0	0·8	–	1·8	0·5
SSE	16·5	2·1	0·7	–	1·8	–
SE	18·2	2·5	0·9	–	2·0	–
SSE	24·1	3·1	1·0	–	0·7	–
S	7·2	2·8	0·9	–	0·8	0·6
SSW	–	1·7	0·6	–	0·5	–
SW	–	1·6	0·6	–	–	–
SWW	–	1·4	0·6	–	–	–
W	–	1·3	0·6	–	–	–
NWW	–	0·7	0·7	–	–	–
NW	–	2·1	0·6	–	–	–
NNW	–	1·5	1·0	–	–	–

Waves lower than 0·5 m and frequency of occurrence less than 5% are not included (modified from Wang, 1993).

with monthly average amplitudes ranging from 0·7 to 1·0 m. Over 60% of the waves are from the NE quadrant during the winter, with monthly average amplitudes ranging from 0·5 to 1·3 m (Table 1).

The strong onshore wind accompanying the passage of typhoons is capable of generating *in situ* high-frequency steep waves over the extensive flat, in addition to the swells propagating from offshore. These locally generated waves have a significant influence on the upper intertidal and lower supratidal zones, where both current and wave energy are typically low during calm weather, and the energy of the offshore swell is usually significantly dissipated. Nearly all the supratidal zone is currently protected by dykes constructed for land reclamation, which were generally established once the elevation of the supratidal zone reached approximately the average spring high water level.

METHODOLOGY

The methodology includes two aspects that sought to understand and quantify the deposition and preservation of tidal bedding. The first aspect emphasized *in situ* observations on the modern tidal flat. Selected points were visited daily during low tide to examine deposition and erosion of the previous two tidal cycles. This daily observation was conducted for 17 days from 1–18 June 1992. Frequent sedimentation and erosion observations across an intertidal profile were conducted for 4 months from May to September 1992. The second aspect of the study focused on examination of the vertical characteristics of tidal laminae and bedding, in terms of the numbers of laminae and lamina thickness variations. Knowledge gained from the *in situ* observations was applied to interpret the vertical distribution of tidal bedding and the preservation potential of individual sandy and muddy laminae in cores and trenches.

A profile, perpendicular to the shoreline, across the nearly 4000-m-wide intertidal flat was surveyed using a level. Thirty-five graduated elevation-monitoring rods were established across the profile (Fig. 2). Relative elevations at each rod were recorded during 22 visits spanning the 4-month study period. During neap tides, several of the rods towards the lower intertidal zone were submerged, and the surface elevations could not be measured. Small erosional holes were sometimes observed in the vicinity the elevation rods, and the depth and size of these scour holes varied at different rods. Generally, the scour holes were larger and deeper, typically several tens of centimetres in diameter and 5–10 cm deep, towards the lower intertidal zone and became smaller, less

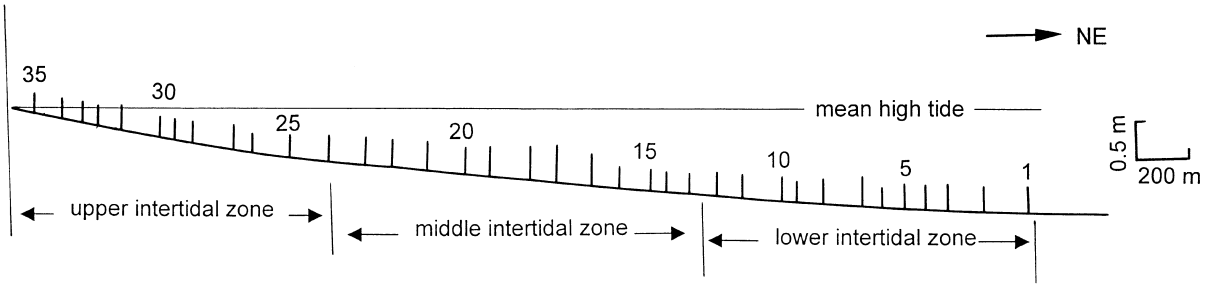

Fig. 2. Tidal-flat profile at Donghai Farm on the southern flank of the Yangtze delta, and locations of the 35 elevation rods. Every fifth elevation rod is labelled.

than 20 cm in diameter and 3 cm deep, towards the upper intertidal zone. A flat steel ruler was used to measure the level of the adjacent sediment surface relative to the elevation rod, regardless of the existence of the scour hole. Therefore, the elevations obtained during the rod monitoring represented an average of the nearby flat, rather than the sediment level at the rod. In the case of the presence of ripples, the data represent an average of the elevation of ripple crests. All the elevations were referred to the first day of measurement, and therefore represent deposition or erosion compared with the situation at the beginning of the monitoring.

Two thin plastic plates, 40 cm long, 40 cm wide and 2 mm thick, were used to monitor the daily sedimentation rate. The plates were placed on the surface of the flat in the vicinity of elevation rod no. 24 in the middle intertidal zone (Fig. 2). The thin plates were placed flush with the average sediment surface, and their surfaces were sanded to increase the roughness. Plate 1 was left in place for a period of 17 days from 1 to 18 June 1992, and one observation was made on 18 June. The objective for monitoring plate 1 was to obtain short-term information without daily disturbance. Sedimentation on plate 2 was measured daily, or every 2 days in cases influenced by poor weather conditions. The thickness of sedimentation was measured by probing a steel ruler down to the plate. The thickness measurements were taken randomly at 12 different points on the plate, and an average value was then used to represent the thickness of sedimentation. The same procedure was followed to ensure the comparability of each measurement. The accuracy of the steel ruler was within 1 mm. The average thickness was influenced by the presence of surficial sedimentary structures, which were typically less than 0·5 cm in relief during the monitoring period, and the purpose of the 12 measurements was to average out these surface ripples. Plate 2 was cleaned after each measurement and redeployed nearby. The objective of the plate 2 experiment was to quantify daily sedimentation rate and the number of laminae formed. Comparison between the sum of the daily measurements and the single 17-day measurement provided information on short-term preservation potential. In other words, if the preservation potential is 100%, the sum of the 17 individual daily sedimentation measurements should equal the deposition measured on the 17-day plate. Plates 1 and 2 were deployed approximately 2 m apart to minimize regional variation. It was assumed that the sanded rough surface of the plates had a negligible influence on sedimentation and preservation, when compared with the natural surface. The fact that plate 2 was covered by sediment and no apparent differences in surface elevation and sedimentary features were observed during each measurement confirms that the above assumption is reasonable. The 17-day monitoring was conducted during calm weather conditions. Waves reported from the Ship Observation Station during the 17-day period were lower than 1·5 m.

Characteristics of tidal bedding (e.g. rhythmic muddy–sandy laminae, lateral extent and thickness variation of individual laminae) were studied in a trench and three cores (Fig. 1). Field observation of tidal bedding in the trench concentrated on the lateral extent and thickness variation of the bedding. In order to quantify the variation in lamina thickness for use in time-series analyses, it is essential to have an adequate lateral extent and uniform thickness in order to minimize irregular local variation. Grain-size analysis of samples from the modern tidal flat was conducted using the method described by Folk & Ward (1957). The sediment was wet-sieved into two fractions using a 4-ϕ sieve. The coarser fraction was analysed by sieving, and the finer fraction was analysed using the pipette method.

RESULTS AND DISCUSSION

The present field observations were conducted in the intertidal zone along an open coast. Although the term tidal flat is used in the previous discussion to indicate a general setting, it is important to note that the present results may not be directly applicable to or comparable with studies in subtidal or supratidal zones. Also, the lack of tidal channels differentiates this study from those conducted in estuaries (e.g. Boersma & Terwindt, 1981; Dalrymple & Makino, 1989; Dalrymple *et al.*, 1991; Shi, 1991) where the influence of tidal channels is significant.

Characteristics of the tidal flat deposits and terminology used in this paper

Sediment samples were collected from individual sandy and muddy laminae in the trench. As expected, mean grain size of individual laminae in the lower intertidal zone was generally coarser than that in the upper intertidal zone (Table 2). A considerable difference in mean grain size, ranging from approximately 1·2 to 2·4 ϕ units, was measured between adjacent sandy and muddy laminae. Although the major fraction of the sediment is silt, the terms sandy and muddy are used here for convenience of discussion in describing the grain-size differences between adjacent laminae.

Two different groupings of sandy and muddy laminae were distinguished (Fig. 3): groups with generally thicker sandy laminae than adjacent groups are termed sand-dominated layers (1 in Fig. 3), while groups with generally thinner sandy laminae than adjacent groups are referred to as mud-dominated layers (2 in Fig. 3). Although determination of the exact boundaries between sand- and mud-dominated layers was somewhat subjective, the overall differences between adjacent sand- and mud-dominated layers were easily apparent. The thickness and number of sandy and muddy laminae in each sand- or mud-dominated layer were not necessarily identical. As discussed in the following section, the deposition and preservation of the mud- and sand-dominated layers are controlled by different mechanisms.

Grain-size analyses using thin slices of sediment across individual sand- and mud-dominated layers indicated that the mean grain size of sand-dominated layers was coarser than that of adjacent mud-dominated layers (Table 3). Again, this comparison emphasizes the difference between adjacent layers, as the mean grain size of a mud-dominated layer in the lower intertidal zone may be coarser than that of a sand-dominated layer in the upper intertidal zone (Table 3).

Monitoring of sedimentation and preservation potential

Sedimentation monitoring on the tidal flat south of the Yangtze River mouth was conducted at three different timescales. The objectives were to estimate and compare fortnightly, seasonal and centennial sedimentation rates and preservation potential. Factors that control the preservation of the intertidal deposits along this open-coastal tidal flat are also discussed.

Short-term monitoring

The objective of the short-term monitoring was to quantify sedimentation rate and preservation potential under calm weather conditions during one spring–neap tidal cycle. Four daily and two twice-daily sedimentation rates were measured (Table 4). As shown in the tidal curve during the 17-day experiment (Fig. 4), spring tides occurred around 2 and 14 June, and neap tides occurred around 7 June. The semi-diurnal tides were not

Table 2. Grain-size variations between adjacent sandy and muddy laminae in the intertidal zone (samples from core T27).

Intertidal zones	Lamination	Grain-size composition (%)			Mean grain size ϕ (mm)	Standard deviation δ_I (ϕ)
		Fine sand (>4ϕ)	Silt (4–8ϕ)	Clay (<8ϕ)		
Upper: average of four samples	Mud laminae	0·61	65·71	33·68	7·90 (0·004)	2·83
	Sand laminae	0·95	91·73	7·32	5·49 (0·022)	1·65
Middle: average of seven samples	Mud laminae	7·08	67·92	25·00	5·96 (0·016)	2·41
	Sand laminae	24·23	69·33	6·44	4·80 (0·036)	1·27
Lower: average of five samples	Mud laminae	19·85	61·88	18·26	5·84 (0·017)	2·69
	Sand laminae	33·16	65·48	1·36	4·00 (0·063)	0·93

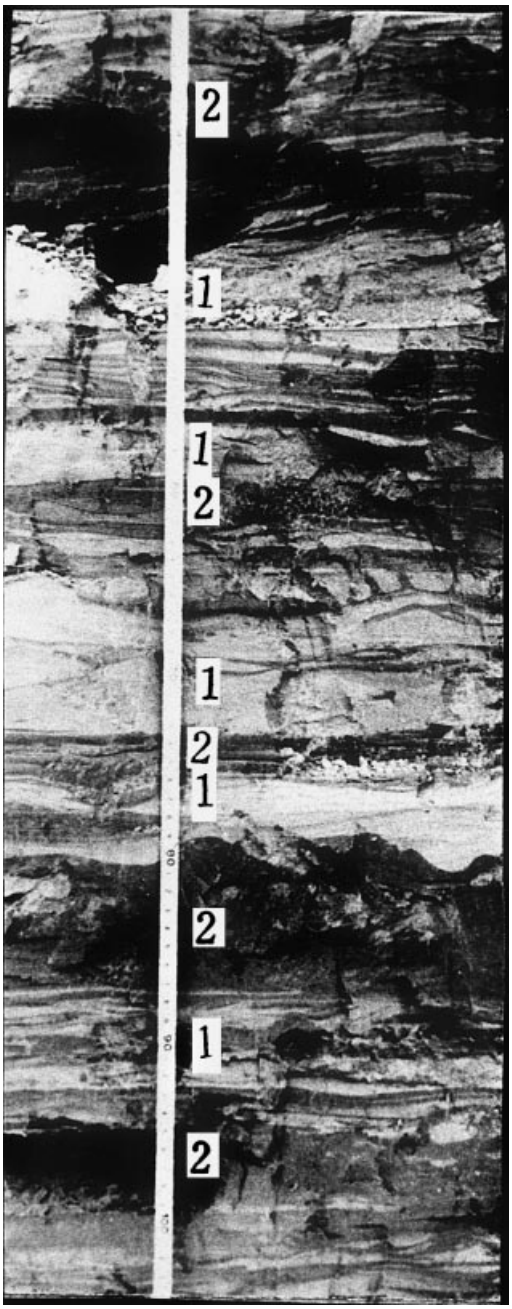

Fig. 3. Different grouping patterns of tidal bedding. 1 denotes a sand-dominated layer, and 2 denotes a mud-dominated layer.

symmetrical, with one tidal range being significantly greater than the other. The sedimentation rates were measured in terms of total thickness and total number of sandy and muddy laminae over time. The daily plate could not be recovered during six visits of the 17-day study period, and four visits had to be cancelled because of rain. Despite the considerable gap in the daily data, the eight daily and twice-daily measurements were extrapolated to compare with the results obtained from the 17-day plate.

Twelve laminae with a total thickness of 75 mm were measured on the 17-day plate. The sum of the six measurements on the daily plate yielded 24 laminae with a total cumulative thickness of 179 mm over an 8-day period (Table 4). A linear relationship between the cumulative number of laminae and the cumulative number of days (Fig. 5),was given by:

$$y = 2{\cdot}92x \quad (1)$$

where y is the cumulative number of laminae, and x is the cumulative number of days. The correlation coefficient r^2 equals 0·99, indicating a strong linear relationship significant at the 0·001% level. The cumulative thickness z was also linearly related to the cumulative number of days (Fig. 5):

$$z = 22{\cdot}22x \quad (2)$$

where z is the cumulative thickness in mm. The correlation coefficient r^2 equals 0·98, also indicating a significant linear relationship at the 0·02% level.

Using Eqs 1 and 2 obtained from the daily data, a 17-day ($x = 17$) total sedimentation thickness was calculated. The calculated 17-day deposition was 378 mm with 50 sandy and muddy laminae. Thus, the uninterrupted 17-day sedimentation was 20% of the extrapolated daily sum in terms of thickness (75 mm vs. 378 mm), or 24% in terms of total number of laminae (12 vs. 50). This indicates that not all the daily sedimentation was preserved even under calm weather conditions. The lower thickness percentage, 20% vs. 24%, might indicate that laminae formed during a previous tidal cycle, or part of a tidal cycle, may be partially eroded and/or reworked by the following tidal cycle. The assumption of 100% preservation potential of tidal bedding is therefore not supported by the present monitoring along an open-coast tidal flat, even under calm weather conditions for a short period of time.

It is generally accepted that four laminae may theoretically be deposited during one tidal cycle (e.g. Li *et al.*, 1965; Allen, 1985; Shi & Chen, 1996). Two sandy laminae may be formed during flood and ebb phases, and two muddy laminae deposited during high- and low-tide slack water. During the 17 days of monitoring, there were 33 tidal cycles (Fig. 4). Based on the above theoretical understanding, 132 laminae could be deposited if the laminae formed in the previous tidal

Table 3. Grain-size differences between adjacent sand- and mud-dominated layers (samples from the trench).

Intertidal zones	Layer	Sand (%)	Silt (%)	Clay (%)	Mean size ϕ (mm)	Standard deviation δ_I (ϕ)
Upper: average of three samples	Mud-dominated	0·13	74·84	25·03	6·81 (0·009)	2·66
	Sand-dominated	0·29	85·69	14·02	5·76 (0·018)	1·92
Middle: average of two samples	Mud-dominated	0·37	82·69	16·94	5·81 (0·018)	2·08
	Sand-dominated	1·18	94·28	4·54	4·07 (0·060)	1·07
Lower: one sample	Mud-dominated	9·43	81·12	9·46	5·30 (0·025)	1·47
	Sand-dominated	10·89	83·20	5·91	4·99 (0·031)	1·15

Table 4. Total thickness and number of laminae measured on the daily and 17-day plates at the Donghai Farm profile.

Observation approach	No.	Observation date	Sedimentation duration (day)	No. of laminae	Thickness (mm)	Sedimentation rate (mm day^{-1})
Daily plate	1	06/01–06/02	1	2	12	12
	2	06/11–06/12	1	4	20	20
	3	06/12–06/14	2	6	42	21
	4	06/14–06/15	1	2	45	45
	5	06/15–06/17	2	6	43	22
	6	06/17–06/18	1	4	17	17
	Total		8	24	179	22
17-day plate		06/01–06/18	17	12	75	4

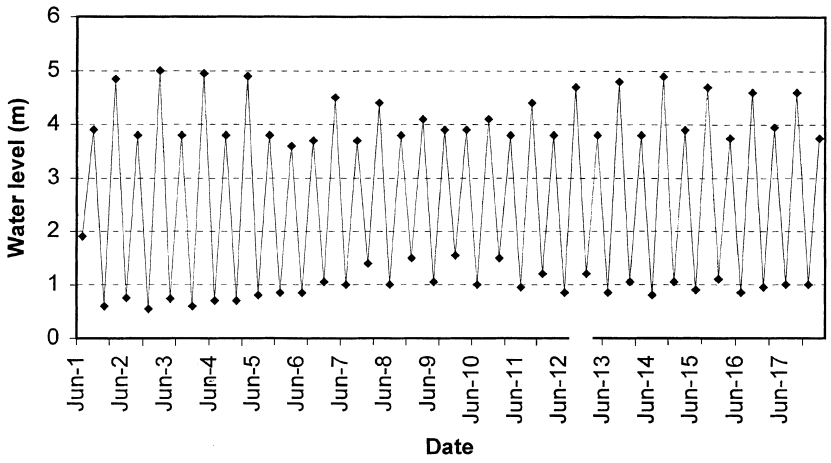

Fig. 4. Tidal curve during the 17-day monitoring period, June 1992.

cycles were not eroded, i.e. with 100% preservation potential. Comparison between the results from the 17-day monitoring (12 laminae) and the theoretical estimate (132 laminae) indicates that only approximately 9% of the laminae were preserved.

The short-term monitoring spanned one spring–neap tidal cycle (Fig. 4). No apparent trend of lamina thickness variation was observed from the daily plate experiments, as also indicated by the significant linear relationship between time and both cumulative thickness and number of laminae. The daily sedimentation rates were rather uniform ranging from 17 to 22 mm day^{-1}, except for two abnormal values of 12 and 45 mm day^{-1}, both measured during spring tides (Table 4). Field observation indicated that the laminae deposited during spring tides were not significantly thicker than those deposited during neap tides. Although accurate measurement of lamina thickness on the 17-day plate was difficult on account of the soft nature of the sediment, no apparent trend in thickness variation was observed. In other words, the present short-term

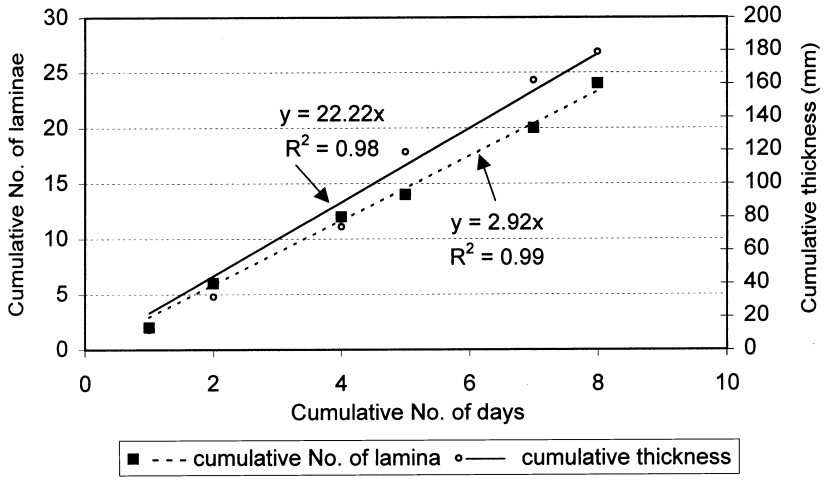

Fig. 5. Cumulative thickness and cumulative number of laminae over time.

data do not support the contention that relatively thick, sandy laminae correspond to spring tides and thin, sandy laminae correspond to neap tides. Also, because of the considerable asymmetry of the semi-diurnal tides, the smaller tidal range during spring tides was similar to the larger tidal range during neap tides (Fig. 4). This spring–neap controlled lamina thickness variation is fundamental for the interpretation of the 14-day period identified from many time-series analysis (e.g. Yang & Nio, 1985).

Mid-term monitoring

The objective of the mid-term monitoring, spanning a period of nearly 4 months, was to identify the impact of high-energy storm events. The monitoring was conducted from May (pre-typhoon) to September (mid-typhoon season) using the series of 35 elevation rods. Overall, the intertidal zone was accreting during the studied calm weather season (Fig. 6), as indicated by the average elevation measurements at all the rods. During the studied storm season, net erosion (elevation decrease) was measured. For the convenience of discussion, the calm and stormy weather season was divided somewhat subjectively by the first significant typhoon impact in the study area, which occurred on 10 August 1992. The frequent observations throughout the 4-month period indicated that the tidal flat was generally muddier in the calm weather season than during the stormy season. The changes in average elevation were not related to the spring–neap tidal cycles, but were closely related to high wave events (Fig. 6).

Tidal-flat responses to the passage of the first major typhoon (typhoon no. 9216) over the study area, from 30 August to 1 September, were

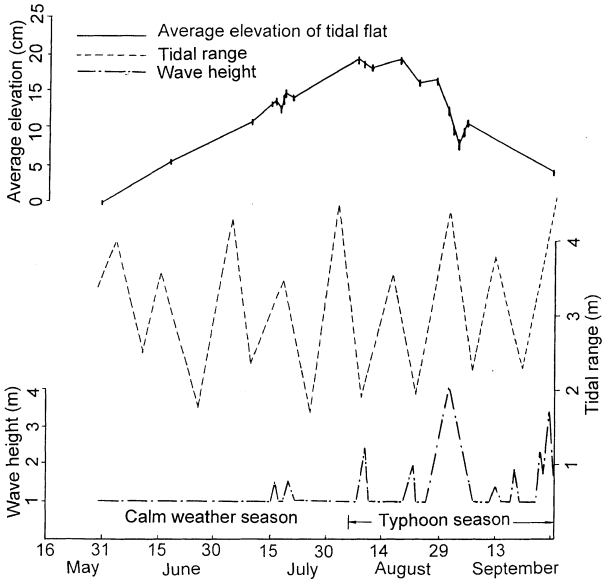

Fig. 6. Average elevation change at Donghai Farm on the southern flank of the Yangtze delta, spring–neap tidal cycles and wave heights observed at the Ship Observation Station during the 4-month study. Wave heights lower than 1 m were neglected.

examined. A thick sandy lamina, overlying the mud-dominated layer present before the typhoon season, was measured immediately after the passage of the typhoon. The top sandy lamina was generally thicker in the lower to middle intertidal zone than that in the upper intertidal zone (Fig. 7). This storm-related sandy lamina was much thicker than the sandy laminae deposited during the calm weather season. The thickness of the top sandy lamina was measured from the underlying muddy lamina at four points near elevation rods no. 14 and 29 (not in the scour hole). A top muddy lamina, if one existed, was not included in the measurement. During stormy

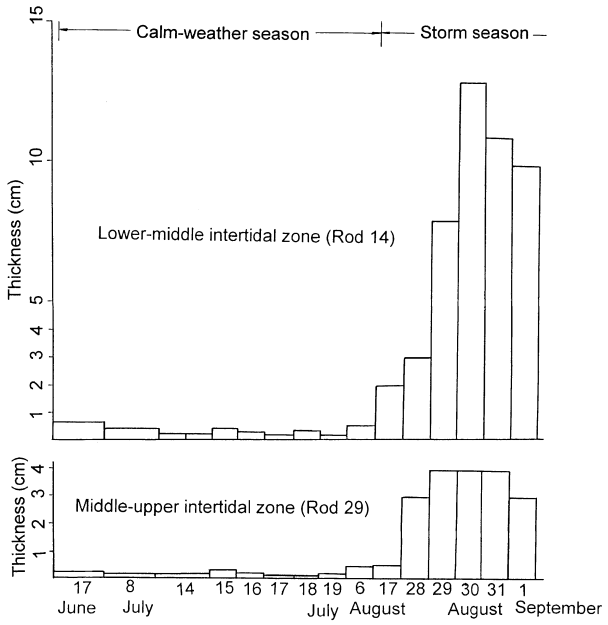

Fig. 7. Thickness of the top sandy lamina in upper (rod no. 29) and middle (rod no. 14) intertidal zones. Note that the time intervals of measurements were not uniform.

days when active sediment resuspension occurred, it was very likely that the deposits of the previous day would be reworked and redeposited. Such was the case for the thick sandy lamina measured during 28–31 August (Fig. 7). During the four consecutive days, only one thick sandy lamina was observed overlying a mud-dominated layer, indicating that the lamina deposited during the previous day was reworked and redeposited. The degree and manner of reworking is beyond the scope of the present study.

On 2 and 3 September, shortly after the passage of typhoon no. 9216, accretion of the tidal flat was measured at the elevation rods (Fig. 6). Alternations of thin muddy and sandy laminae were observed overlying the thick sandy lamina of the storm deposit. The study site was revisited after the second significant typhoon (typhoon no. 9219) impact on 26 and 27 September 1992. The thin muddy and sandy laminae deposited between the two typhoons were completely eroded, resulting in a considerable lowering of the overall tidal-flat elevation (Fig. 6).

The results obtained from the mid-term monitoring, although limited in temporal coverage, indicate that the mud-dominated layers described above (Fig. 3) probably correspond to calm weather deposition, while the sand-dominated layers are related to high-energy storm events. The accumulation of part of a mud-dominated layer was observed during the short-term monitoring under calm weather conditions. No relatively thick sandy lamina was measured during the calm weather monitoring, as indicated by the generally thin top sandy lamina measured before the storm season (Fig. 7).

In summary, in contrast to the spring–neap cycle interpretation of variations in lamina thickness, this mid-term sedimentation and erosion monitoring on an open-coast tidal flat suggests that the thick–thin alternation of sandy laminae in tidal-flat deposits may also be event driven. Deposition of a relatively thicker sandy lamina was directly related to the high-energy wave events induced by the passage of a typhoon, instead of during spring-tide conditions.

Long-term monitoring

Long-term monitoring, with the objective of determining the centennial sedimentation rate and preservation potential was based primarily on the analysis of sedimentary structures in cores and trenches. A shoreline progradation rate was estimated from the construction of four different phases of dykes from 1960 to 1985 (Table 5). As a dyke was usually constructed as soon as the upper tidal-flat level reached spring high water level, an average rate of shoreline progradation can be estimated by dividing the distance between the dykes by the time interval between construction. In this manner, an average rate of shoreline progradation of 41 m per year was estimated from the four phases of dyke construction. Assuming that shoreline progradation rate and the average width of the intertidal zone have remained reasonably constant during the last century, it would therefore take approximately 100 years for the shoreline to prograde across the entire 4000-m-wide intertidal zone. The thickness of a complete tidal sequence equals approximately 4·0 m, as determined by the present average spring tidal range, and agrees with the elevation difference from the vegetation line to the approximate mean spring low water. A long-term sedimentation rate of 4 cm per year was therefore estimated.

Based on Pb^{210} dating, sedimentation rates ranging from 2·2 to 3·8 cm per year were obtained at the Donghai Farm tidal flat (Li, 1993; Li & Li, 1994), adjacent to the study area. Sedimentation rates obtained using the Pb^{210} method from a number of other locations on the Yangtze delta typically range from 2 to 4 cm per year, with a minimum of 0·3 cm per year (Li *et al.*, 1992, 1993; Li & Xie, 1993; Xie *et al.*, 1994, 1997).

Table 5. Average shoreline progradation rate estimated from the four phases of dyke construction.

Dyke name	Year of construction	Years between dyke construction	Average progradation distance (m)	Progradation rate (m year^{-1})	Average progradation rate (m year^{-1})
People's Dyke	1960				
		14	440	32	
Victory Dyke	1974				
		5	330	66	41
79 Dyke	1979				
		6	260	43	
85 Dyke	1985				

The above estimate of shoreline progradation rate using phases of dyke construction may involve considerable uncertainty, mostly associated with the engineering determination of the dyke location. However, accurate assessment of shoreline change at an extremely gentle tidal flat with up to 4·0 m tidal range is difficult. Aerial photos have only become available in recent years, and the recent rates of shoreline change are strongly influenced by increased human activity. It is therefore believed that the above estimates of long-term shoreline change using dyke construction provide an acceptable approximation. Based on field experience and comparison with estimates from Pb^{210} dating, a 20–30% uncertainty in the calculation of sedimentation rate was estimated.

The numbers of sand- and mud-dominated layers were counted in the three cores and one trench (Fig. 1). The trench was located in the present supratidal zone slightly landward of the vegetation line. The studied sections were interpreted as intertidal deposits based on regional trends in palaeogeography and stratigraphic evolution (Stanley & Chen, 1993; Chen & Stanley, 1993; Chen, 1998) and assemblages of sedimentary structures and microfossils (Li & Wang, 1998).

The numbers of sand-dominated layers counted in the three cores are listed in Table 6. As discussed earlier, the sand-dominated layers became more difficult to distinguish towards both the lower and the upper intertidal zones. The uncertainty associated with the determination of the sand-dominated layers is estimated to be between 10% and 20%. Based on the above discussion, it is reasonable to assume that a complete intertidal sequence should be 4 m thick and represent approximately 100 years of sedimentation. The lengths of two of the cores were slightly less than 4 m. In order to obtain the number of sand-dominated layers over a complete intertidal section, the results were extrapolated linearly to represent a 4-m section (Table 6). An average of 32 sand-dominated layers was obtained in the three cores.

From 1949 to 1989, 100 summer high-energy events, including typhoons and strong tropical cyclones, impacted upon the studied coast, averaging 2·5 events per year (Wang, 1993). Strong winter cold fronts, which occur five to eight times per year, also have a significant impact. However, as most of the cold fronts approach from the north-west, their influence on the coast is limited because they move from land to sea. Cold fronts from the north-east are relatively rare but have a much more significant impact in terms of generating high waves. The north-east cold fronts are capable of generating waves with energy levels similar to those of typhoons and/or strong tropical cyclones. Previous studies have indicated that, on average, one strong cold front from the north-east impacts the coast each year (Sun, 1981;

Table 6. Numbers of sand-dominated layers in the three cores and trench.

Core	Measured thickness (m)	No. of sand-dominated layers	No. of sand-dominated layers calculated by linear extrapolation to a 4-m section
T28	4·0	28	28
T26	3·3	28	34
T27	3·5	30	34
Trench Lg-1	1·73	12	28

Zhu *et al.*, 1989). Combining the passages of typhoons, strong tropical cyclones and cold fronts, it was estimated that the studied coast was impacted by high-energy storm events, on average, 3·5 times per year. Thus, in the 100 years during which a complete sequence of intertidal deposits may develop, the coast could have experienced of the order of 350 storm impacts.

If the passage of each storm resulted in the deposition of one sand-dominated layer and every layer was preserved, in 100 years some 350 sand-dominated layers would be deposited. Therefore, the 32 sand-dominated layers that were counted in the cores suggest a 9% preservation potential for the storm deposits. As discussed in the previous section, the second or possibly the third typhoon during the same storm season may not result in new deposits overlying the previous storm deposits. Instead, the thick, storm-related, sandy laminae along with the thin sandy and muddy laminae alternations deposited between storms may simply be reworked.

Counting of individual laminae was conducted in core T27 (Fig. 1). Three hundred and eighty-five (385) laminae were counted in the upper intertidal zone, 109 in the middle intertidal zone and 52 in the lower intertidal zone, with a total of 546 laminae. Distinction among upper, middle and lower intertidal zones was based on characteristics of the sedimentary structures (Reineck & Singh, 1980) sediment grain size and the general trend of lamina thickness (Li & Wang, 1998). The upper intertidal zone is characterized by relatively fine sediment with thicker muddy laminae. Lenticular bedding is common in the upper intertidal zone, while the lower intertidal zone is characterized by coarser sediment and thicker sandy laminae. Flaser bedding is common in the lower intertidal zone, and wavy bedding is common in the middle intertidal zone. Although the exact boundaries between the upper, middle and lower intertidal zones were somewhat subjective, the overall trend was apparent. In reality, there are no abrupt boundaries between the upper, middle and lower intertidal zones, but these terms provide convenience for description. A 15–25% uncertainty in counting the number of laminae was estimated on account of the subjectiveness of the boundaries.

The core section was 3·5 m thick. Linear extrapolation to the complete 4-m intertidal sequence yields an estimate of 624 sandy and muddy laminae. Under a typical semi-diurnal tidal regime, there are 70 645 tidal cycles in 100 years. Thus, from the theoretical understanding of four laminae per tidal cycle, 282 580 laminae could be deposited. The 624 laminae that were actually preserved therefore represent 0·2% of the potential accumulation. In other words, the overall preservation potential of laminae in a 100-year period is of the order of 0·2%, and more than 99% has been either eroded or reworked, leaving no sedimentary record. The number of laminae decreases significantly from the upper intertidal zone (385) to the lower intertidal zone (52), suggesting that the preservation potential of individual laminae is significantly influenced by wave energy.

In summary, the short-term observation during a spring–neap tidal cycle suggests a preservation potential of about 10% on a fortnightly scale. Although these data are limited in temporal and spatial coverage, the results indicate that complete preservation of the deposits from a spring–neap tidal cycle is not likely, even during a very short period of time and not considering erosion by high-energy events. During a period of 100 years, a preservation potential of lamina of the order of 0·2% was obtained for open-coast intertidal deposits. Seasonal monitoring indicates that the mud-dominated layers are probably deposited during calm weather conditions, while sand-dominated layers probably accumulate during storm seasons. During the 100-year period, storm deposits described in terms of sand-dominated layers have a much higher preservation potential of approximately 10%, compared with overall laminae preservation of 0·2%. Although the above estimates of preservation potential were obtained in terms of the number of laminae, they should have valuable implications in estimating sedimentation rates in tidal-flat deposits.

CONCLUSIONS

Waves, especially high-energy waves generated by storm events, have a significant influence on the sedimentation and preservation of intertidal deposits along an open-coast tidal flat. Short- and mid-term monitoring indicated that the thickness variation in sandy laminae on an open-coast intertidal zone is not related to spring–neap tidal cycles, but is directly related to storm activity. The mud-dominated layers containing thin sandy laminae tend to be deposited during calm weather conditions.

One hundred per cent preservation of both the number and the thickness of individual laminae in tidal-flat deposits, which has been assumed in

the interpretation of time-series analysis of laminae thickness variation, was found to be unrealistic along the studied open-coast tidal flat. Preservation potential decreases as timescale increases. During one spring–neap tidal cycle under calm weather conditions, the preservation potential of individual laminae was approximately 9%. However, over a period of 100 years, the preservation potential of individual laminae decreased to about 0·2%. The preservation potential of storm-induced, sand-dominated layers during the 100-year period was found to be of the order of 10%, much higher than the 0·2% of the individual sandy and muddy laminae.

ACKNOWLEDGEMENTS

This research was supported by the National Natural Science Foundation of China (grant no. 49677288). We thank Q. Chen, C. Han and X. Cai for their assistance in the field work, and M. Wu, Z. Wang and Kerry Lyle for their assistance in cartography and photography. An earlier draft of this paper was reviewed by David Pepper. We are grateful to Drs Clare Davies, Robert Dalrymple and Jim Best for critical and constructive reviews of this paper.

REFERENCES

Allen, J.R.L. (1985) *Principles of Physical Sedimentology*. George Allen & Unwin, London, Boston, Sydney.

Boersma, J.R. (1969) Internal structures of some tidal megaripples on a shoal in the Westerschelde estuary, the Netherlands. *Geol. Mijnbouw*, **48,** 409–414.

Boersma, J.R. and **Terwindt, J.H.J.** (1981) Neap–spring tide sequences of intertidal shoal deposits in a mesotidal estuary. *Sedimentology*, **28,** 151–170.

Chen, X. (1998) Changjian (Yangtze) River delta, China. *J. Coastal Res.*, **14,** 838–858.

Chen, Z. and **Stanley, D.J.** (1993) Yangtze delta, eastern China: 2. Late Quaternary subsidence and deformation. *Mar. Geol.*, **112,** 13–21.

Dalrymple, R.W. and **Makino, Y.** (1989) Description and genesis of tidal bedding in the Cobequid Bay–Salmon River Estuary, Bay of Fundy, Canada. In: *Sedimentary Facies of the Active Plate Margin* (Eds A. Taira and F. Masuda), pp. 151–177. Terra Scientific, Tokyo.

Dalrymple, R.W., Makino, Y. and **Zaitlin, B.A.** (1991) Temporal and spatial patterns of rhythmite deposition on mud flat sedimentation in the macrotidal Cobequid Bay–Salmon River estuary, Bay of Fundy, Canada. In: *Clastic Tidal Sedimentation* (Eds D.G. Smith, G.E. Reinson, A. Zaitlin and R.A. Rahmani), *Can. Soc. Petrol. Geol., Mem.*, **16,** 137–160.

Folk, R.L. and **Ward, W.L.** (1957) Brazos river bar, a study in the significance of grain size parameters. *J. Sedim. Petrol.*, **27,** 3–27.

Kuecher, G.J., Woodland, B.G. and **Broadhurst, F.M.** (1990) Evidence of deposition from individual tides and of tidal cycles from the Francies Creek Shale. *Sedim. Geol.*, **68,** 211–221.

Kvale, E.P. and **Archer, A.W.** (1990) Tidal deposits associated with low sulfur coals, Brazil FM. (Lower Pennsylvanian), Indiana. *J. Sedim. Petrol.*, **60,** 563–574.

Kvale, E.P., Archer, A.W. and **Johnson, H.R.** (1989) Daily, monthly, and yearly tidal cycles within laminated siltstones of the Masfield Formation of Indiana. *Geology*, **17,** 365–368.

Li, C. (1986) Deltaic sedimentation. In: *Modern Sedimentation in Coastal and Nearshore Zone of China* (Ed. M.E. Ren), pp. 253–378. China Ocean Press and Springer-Verlag, Beijing, Berlin, Heidelberg, New York, Tokyo.

Li, T. (1993) *Study on Tidal Flat Sequence and Storm Deposit of Southern Flank of the Yangtze Delta.* Unpublished PhD Thesis, Marine Geology Department, Tongji University, Shanghai, China, 51 pp (in Chinese).

Li, T. and **Li, C.** (1994) Tidal flat sedimentation and event. *Chinese Sci. Bull.*, **39,** 223–228 (in Chinese with English abstract).

Li, C. and **Wang, P.** (1998) *Late Quaternary Stratigraphy of the Yangtze Delta.* China Science Press, Beijing, 222 pp (in Chinese).

Li, Y. and **Xie, Q.** (1993) Zonation of sediment and sedimentation rate on Andong tidal flat in Hangzhou Bay, China. *Donghai Mar. Sci.*, **11,** 21–33 (in Chinese with English abstract).

Li, C., Yang, X., Zhuan, Z., Jian, Q. and **Wu, S.** (1965) Formation and evolution of the intertidal mudflat. *J. Shangdong College Oceanogr.*, **2,** 21–31 (in Chinese with English abstract).

Li, C., Guo, X. and **Xu, S.** (1979) Characteristics and distribution of Holocene sand bodies in the Yangtze Delta. *Acta Oceanol. Sinica*, **1,** 252–268 (in Chinese with English abstract).

Li, C., Chen, G., Yao, M. and **Wang, P.** (1991) The influences of suspended load on the sedimentation in the coastal zones and continental shelves of China. *Mar. Geol.*, **96,** 341–352.

Li, Y., Pan, S., Shi, X. and **Li, B.** (1992) Sedimentation rate of the tidal flat at the high-suspended load estuary of Geojiang River, Province Zhengjiang, China. *J. Nanjing Univ. (Nat. Sci. Edn),* **28,** 623–631 (in Chinese with English abstract).

Li, Y., Berger, G.W. and **ven Weering, Tj.C.E.** (1993) Pb^{210} as a tracer for the tidal flat sedimentation in the southern Hangzhou Bay. *Donghai Mar. Sci.*, **11,** 34–43 (in Chinese with English abstract).

Miller, D.J. and **Eriksson, K.A.** (1997) Late Mississippian prodeltaic rhythmites in the Appalachian Basin: a hierarchical record of tidal and climatic periodicities. *J. Sedim. Res.*, **67,** 653–660.

Reineck, H.E. and **Singh, I.B.** (1980). *Depositional Sedimentary Environments*. Springer-Verlag. New York.

Shi, Z. (1991) Tidal bedding and tidal cyclicities within the intertidal sediments of the Dyfi River estuary, West Wales, UK. *Sedim. Geol.*, **73,** 43–58.

Shi, Z. and **Chen, J.** (1996) Morphodynamics and sediment dynamics on intertidal mudflats in China (1961–94). *Cont. Shelf Res.*, **16,** 1909–1926.

Stanley, D.J. and **Chen, Z.** (1993) Yangtze delta, eastern China. 1. Geometry and subsidence of Holocene depocenter. *Mar. Geol.*, **112,** 1–11.

Sun, X.P. (1981) *Meteorological and Oceanographical Characteristics in the Coastal Zone of China.* China Ocean Press, Beijing, 205 pp (in Chinese).

Tessier, B. (1993) Upper intertidal rhythmites in the Mont-Saint-Michel Bay (NW France): perspectives for paleo-reconstruction. *Mar. Geol.*, **110,** 355–367.

Tessier, B. and **Gigot, P.** (1989) A vertical record of different tidal cyclicities: an example from the Miocene Marine Molasse of Digne. *Sedimentology*, **36,** 767–776.

Visser, M.J. (1980) Neap–spring cycles reflected in Holocene subtidal large-scale bedform deposits: a preliminary note. *Geology*, **8,** 543–546.

Wang, L. (1993) *Climate Condition in the Pudong Development Area, Shanghai.* Technical Report no. 93001. Shanghai Meteorological Bureau, Shanghai, 26 pp (in Chinese).

Xie, Q., Li, B., Xia, S., Li, Y., ven Weering, Tj. C.E. and **Berger, G.W.** (1994) Spatial and temporal variations of tidal flat in the Oujiang estuary in China. *Acta Geogr. Sinica*, **49,** 509–516 (in Chinese with English abstract).

Xia, X., Xie, Q., Li, Y. and **Li, B.** (1997) Cyclicity of mud tidal flat in coastal bays. *Acta Oceanol. Sinica*, **19,** 99–108 (in Chinese with English abstract).

Yang, C. and **Nio, S.** (1985) The estimation of palaeohydrodynamic processes from subtidal deposits using time-series analysis methods. *Sedimentology*, **32,** 41–57.

Zhu, H., Yuan, C., Mao, Z. and **Wang, S.** (1989) The wave characteristics and their relationship with winds at the Yangtze river mouth area. In: *Dynamic Process and Geomorphological Evolution of the Yangtze Estuary* (Eds J. Chen, H. Shen and C. Yuan), pp. 166–177. Shanghai Science and Technology Press, Shanghai (in Chinese).

Manuscript received 30 April 1999;
revision accepted 1 March 2000.